Benavente Martínez, R.; Salvador Moya, MD.; Martínez-Amesti, A.; Fernández, A.; Borrell Tomás, MA. (2016). Effect of sintering technology in beta-eucryptite ceramics: Influence on fatigue life and effect of microcracks. Materials Science and Engineering: A. 651:668-674. doi:10.1016/j.msea.2015.11.013.

Effect of sintering technology in β-eucryptite ceramics: Influence on fatigue life and effect of microcracks

Rut Benavente[1*], María Dolores Salvador[1], Ana Martínez-Amesti[2], Adolfo Fernández[3] and Amparo Borrell[1]

[1]*Instituto de Tecnología de Materiales (ITM), Universitat Politècnica de València, Camino de Vera, s/n, 46022 Valencia, Spain*

[2]*Universidad del País Vasco (UPV/EHU), Facultad de Ciencia y Tecnología, SGIker. Microscopia Electrónica y Microanálisis de Materiales, Barrio Sarriena, s/n, 48940 Leioa (Vizcaya), Spain*

[3]*Centro de Investigación en Nanomateriales y Nanotecnología (CINN) (CSIC-UO-PA), Avenida de la Vega 4-6, 33940 El Entrego (Asturias), Spain*

*Corresponding author: Instituto de Tecnología de Materiales (ITM), Universitat Politècnica de València, Camino de Vera s/n, 46022, Valencia, Spain. Tel.: +34963877007; Fax: +34963877629. E-mail address: rutbmr@upvnet.upv.es.

Abstract

β-eucryptite ceramics with low negative or near-zero coefficient of thermal expansion (CTE) with excellent mechanical properties, such as Young's modulus ≥ 100 GPa, have attracted attention for many important industrial applications. The extremely anisotropic thermal expansion behaviour of this material leads to thermal residual stresses, and causes spontaneous microcracking. These microcracks cause large negative CTE with mechanical weaknesses. The appearance of microcracks is due to different factors. The most important are prolonged sintering time and heating source used.

The present work shows experimentally the evolution of grain microcracks and residual stresses of the sintered β-eucryptite material going through many thermal fatigue cycles (~3600). The effect of stresses applied on β-eucryptite crystals due to the thermal cycling could be considered for explaining the small change observed of β-eucryptite to β-spodumene phase, which is higher in the samples obtained by microwave sintering. Therefore, the study of residual stresses has suggested that the heating source employed, such as conventional or microwave, has a great influence on thermal fatigue life and the final mechanical and thermal properties. The microwave heating has a significant impact on β-eucryptite materials lifetime.

Keywords: Microwave sintering; β-eucryptite; Mechanical properties; Thermal fatigue; Microcracking

1. Introduction

Microcracked ceramic materials possess superior thermal shock resistance, owing to their unique physical and thermo-mechanical properties [1]. Microcracking is often displayed in ceramics with anisotropic coefficients of thermal expansion, leading to grain-level internal stresses that cause bond rupture and spontaneous micro-fracture [2]. Thermal misfit strains in such ceramics materials, due to the high thermal expansion mismatch and anisotropy, may reach sufficiently high values to cause spontaneous microcracking. Such cracking associated with thermal misfit strains in ceramics, glasses and brittle composites has been observed to occur in a myriad of material systems [3-6].

Lithium aluminosilicate (LAS) ceramic shows extremely anisotropic thermal expansion due to its hexagonal crystal structure [7], resulting in a low or negative coefficient of thermal expansion (CTE) [8]. Accordingly, these ceramics are predominantly used to tailor materials with high resistance to thermal shock and good dimensional stability. β-eucryptite ($LiAlSiO_4$) and β-spodumene ($LiAlSi_2O_6$) [9,10] are the most studied LAS systems. However, it is noteworthy that the β-eucryptite has a more negative CTE in a wide range of temperatures and present higher mechanical properties.

The microcracks have important effects like a very negative coefficient of thermal expansion (CTE), and also decreased mechanical properties, such as hardness and Young's modulus [11]. Therefore, the development and new potential engineering applications of β-eucryptite materials, with null CTE and advanced mechanical properties, are very limited.

Several authors have reported that the microcracking, and therefore thermal expansion, depend on the grain size of β-eucryptite [1,12]. Specifically, when the grain size is larger, the extent of microcracking is greater, leading to a large negative CTE, and vice versa. For example, it has been reported by Pelletant et al. [12] the critical grain size for inducing microcracking in pure β-eucryptite ceramics as a consequence of the thermal expansion anisotropy is less than 2.8 μm. Our previous results show that the microcracking not only depends on the minimum or critical grain size, but also, the sintering methodology is an important factor in their formation [13-15].

Some studies have focused on dimensional stability behavior of these materials over time, with no loads or variable environmental conditions, but there are no previous literature results on the subject regarding mechanical and thermal properties over time in use. Hysteretic temperature effects can have a significant cumulative effect on the

structure due to the large number of thermal cycles that the material may experience in its operational lifetime. Microcracking also could be induced in the crystalline state by thermal treatments [11]. Therefore, the current study aims to know and follow the microcracks formation in β-eucryptite solid-state materials to fabricate cutting-edge materials with different multifunctional applications and, also, increase the service life.

In this work, the samples were fabricated by two different methods, conventional and microwave sintering. Microwave technology of ceramic materials has gained new relevance in the field of sintering and consolidation due to its benefits compared with conventional heating techniques [16-19]. Some of the main advantages of this non-conventional sintering method are, for example: rapid and volumetric heating, reduced processing times, energy efficiency and environmental benefits. This specific heating technique allows obtaining ceramic materials with a unique combination of structural and functional properties [20,21].

In the present investigation, microcracked structures of β-eucryptite were produced via repeat thermal fatigue cycles, heating-cooling in an electric furnace. The formation of this microcracking and its relationship with the sintering method and the effect on the CTE and mechanical properties is the scope of our study.

2. Materials and methods

2.1. Starting materials

β-eucryptite solid solution powders were synthesized for this study following the route proposed in a previous work (see [8] for details). The chemical compositions of the lithium aluminosilicate (LAS) powder correspond to a Li_2O:Al_2O_3:SiO_2 relation of

1:1.1:2.5 (Compositions LAS8 in [8]). Green samples were prepared by cold isostatic pressing (CIP) at 200 MPa of pressure (15 mm height, 10 mm diameter). The green density was approximately 1.2 g cm^{-3}, i.e. 49% of theoretical density (2.39 g cm^{-3}).

2.2. Thermal cycling

Green samples were sintered in air by pressureless conventional heating process in an electrical furnace (Thermolynetype 46100, Thermo Fisher Scientific, USA) at 1200 ºC with 10 ºC min^{-1} of heating rate and 2 h of holding time at the maximum temperature [13]. On the other hand, a single mode cylindrical cavity operating in the TE_{111} mode with a resonant frequency of 2.45 GHz was selected as the heating cell for microwave sintering [22]. The samples were sintered at 1200 ºC in air with a heating rate of 100 ºC min^{-1} with a short holding time of 10 min [15].

Thermal fatigue cycles were carried out in an electric furnace (Energon S.L., Spain). The oven has a platform that goes up and down allowing the rapid heating and cooling of the samples. Each cycle involves samples heating to 400 ºC for 10 minutes of holding time and cooling with cold air immediately. The cycles number chosen were 800, 1800 and 3600.

2.3. Material characterization

The bulk density of the sintered samples was measured by Archimedes method in distilled water liquid (ASTM C373-88).

The fracture surface sections of the samples have been observed using a field emission gun scanning electron microscope (FE-SEM, HITACHI S-4800, Japan).

Nanomechanical properties such as hardness and Young's modulus of samples were obtained by nanoindentation technique (Model G200, MTS Company, USA). Tests were performed under maximum depth control, 2000 nm, using a Berkovich diamond tip previously calibrated with silica. The contact stiffness (*S*) was determined by Continuous Stiffness Measurement technique (CSM) to calculate the profiles of hardness (*H*) and elastic modulus (*E*) [23]. Amplitude was programmed to 2 nm with 45 Hz of frequency. A matrix with 25 indentations was performed for each sample. In order to ensure the quality of the tip throughout the work, pre- and post- calibration procedures were performed for this indenter ensuring the correct calibration of its function area and correct machine compliance. Previous to the nanoindenter testing, the samples were prepared by metallographic techniques. After cutting (Secotom-15, Struers, Denmark), the surface was lapped and then polished (LaboPol, Struers, Denmark), with a final step with 0.25 µm diamond paste.

The crystalline phases of the bulk ceramic composites were determined by X-ray diffraction. The obtained XRD patterns were indexed using the diffraction files of β-eucryptite (PDF: 870602) and β-espodumene (PDF: 350797). Patterns were obtained from a diffractometer (XRD, BRUKER AXS D5005, Germany) using Cu Kα radiation. The measurements were performed in the 15º-75º range and the step size and time of reading were 0.01º and 2 s, respectively.

Structural refinements were performed using the Rietveld method [24] in the Fullprof programme [25]. The crystallite size (domains over which diffraction is coherent) of the samples was obtained from the peak profile of the diffraction data. Profile fitting was performed using a Thompson-Cox-Hastings pseudo-Voigt function to extract the size broadening (β_{size}) and strain broadening (β_{strain}), which contribute to the integral breadth

(β) of the diffraction peaks. The integral breadth was corrected for instrumental broadening (β_{instr}) to determine the sample broadening (β_{size}, β_{strain}). The instrumental broadening was determined experimentally with diffraction standard, lanthanum hexaboride, LaB_6.

The crystallite sizes were calculated using the Scherrer equation [26], and the obtained strain (expressed in %% units, i.e. per 10.000) corresponds to 1/4 of the apparent strain, as defined by Stokes and Wilson [27]. The following equations relate the crystallite size and strain with the β_{size} and β_{strain}, respectively:

$$Crystallite\ size\ (\text{Å}) = 1/\beta_{size}$$

$$Strain\ (\%\%) = {}^{1}/_{2} \cdot \beta_{tensión} \cdot d_{hkl}$$

β_{size} and β_{strain} were obtained assuming a Lorentzian-Gaussian profile, and β was calculated using the De Keijser formula [28].

Furthermore, the theoretical density was calculated from molecular weight and crystal structure using the following equation.

$$\rho = \frac{Z \cdot Pm \cdot 1.66}{V}$$

Where *Z* is number of asymmetric unit in unit cell, *Pm* is the molecular weight of the compound and *V* is the volume of unit cell.

The coefficient of thermal expansion was checked in a Netzsch DIL-402-C between -100 and +400 ºC.

3. Results and discussion

3.1. Microcracking and grain size

The relative densities of sintered samples obtained by conventional sintering at 1200 ºC with 2h of holding time (CS 1200-2h) and microwave sintered at 1200 ºC during 10 minutes of holding time (MW 1200-10) were 90% and 99% approximately, respectively. The microwave-sintered samples show a relatively high value, close to theoretical density, and enhanced by 9% compared with the CS 1200-2h samples.

To carry out this study, despite the different density values of both samples, we have chosen these materials (CS 1200-2h and MW 1200-10) based on previous study [13], where β-eucryptite material was obtained with glass-free and high mechanical properties by conventional and microwave methods, using the best sintering conditions.

Figure 1 shows the FE-SEM fracture surface of β-eucryptite samples sintered by conventional and microwave technology at 1200 ºC, as-sintered and after undergoing different thermal fatigue cycles (0 to 3600). The difference in microcracks number between both samples before thermal cycling is remarkable. Before subjecting the samples to thermal fatigue cycles, a large number of microcracks was observed in the conventional samples (Figure 1a), but only a few microcracks are observed in samples obtained by microwave (Figure 1b). After thermal cycling process, the appearance of microcracks and their length increases with the number of cycles in all samples. It can be observed, that microcracks go through one grain, approximately, before thermal fatigue, nevertheless, after thermal process, microcracks cross several grains.

As mentioned above, as-sintered microwave material is largely free of cracks. However, as can be seen in Figure 1d and 1f, thermal fatigue tests cause their appearance. It is

widely accepted in the literature that microcracks depend on the grain size of β-eucryptite material, and there is a critical grain size below which microcracks do not occur [1,2,6,12]. Bruno et al. [1] found that different grain sizes induce microcracking at different temperatures (~500 ºC for large grains, 20-30 μm, and 300 ºC for medium grain sizes, 5-10 μm) on cooling, and microstress relaxation occurs at the same temperatures. Shyam et al. [6] demonstrated that grain sizes <4 μm of β-eucryptite material are nominally free of microcracks. Pelletant et al. [12] reported that the critical grain size for spontaneous microcracking is less than 2.8 μm. Other studies revealed that prolonged conventional sintering time (~25 h) introduced microcracks in the sintered samples [11]. However, there are no studies in the literature that show the relationship between grain size and microcracking of β-eucryptite materials obtained by non-conventional sintering techniques, and how this fast heating affects the internal stresses.

Grain size of CS and MW samples are presented in Table 1. It can be observed that the grain size of the β-eucryptite obtained by the conventional method is a little greater than that obtained by the microwave technique. This difference in grain size of the sintered materials by both techniques is maintained throughout thermal cycling, as expected. The final temperature of thermal fatigue tests, 400 ºC, is not enough to cause grain coarsening or an increase in densification. In any case, the grain size achieved in all samples is close to the critical value reported by different authors to begin spontaneous microcracking. Nevertheless, we found a remarkable difference in the amount of microcracks present in as-sintered conventional samples. The considerable difference of sintering time, heating source and heating/cooling rates used in the two sintering methods could drive to obtain samples with different residual internal stresses and, therefore, different microcracking levels.

In a conventional furnace the materials are heated by convection, the surface of particles receives the heat and, therefore, is more reactive. In contrast to convection heating, in a microwave the material absorbs the electromagnetic waves and the heating is volumetric. Due to the microwave energy, sintering occurs due to a "*self-heating*" of the material itself, reaching the maximum temperature in the core, where the greatest concentration of mass is located. The temperature gradient generated in the grains of β-eucryptite is different depending on the sintering method used. This effect could be cause of the different residual internal stresses and, therefore, provoke different microcracking levels.

3.2. Evolution of crystal structure

The internal stresses generated by thermal fatigue to which the sample has been subjected, lead to the grain breaking. The high anisotropy in the crystal structure of the β-eucryptite causes the expansion of a and b axes, while the c axis is contracted. These internal stresses are released by spontaneous rupture of the grain [9]. The microcracks generated continuously open and close upon heating and cooling. Bruno et al. [1] reported that the microcracks reopen only when the thermal stresses exceed the grain strength of the material.

In order to study the composition and the evolution of the crystal structure with thermal fatigue cycling, X-ray diffraction (XRD) measurements were performed. Rietveld method was used to refine the XRD of the CS and MW samples as-sintered and after 3600 thermal fatigue cycles. Figure 2 shows the Rietveld refinement of X-ray diffraction patterns at room temperature. The lattice parameters, unit cell volume,

theoretical density, crystalline strain and the goodness-of-fit parameters obtained from X-ray full-profile refinement are summarized in Table 2.

Furthermore the calculated residual stresses of as-sintered MW samples show a lower percentage of internal stresses than CS samples (CS: 25.34 %%, MW: 21.54 %%), despite being obtained with a higher heating and cooling rate. This could explain that samples with more residual stresses have higher content in microcracks, as can be seen in Figure 1. As-sintered CS samples showed more microcracks (Figure 1a) than MW samples (Figure 1b).

After thermal fatigue, the effect caused by thermal cycling in the samples is different depending on the sintering method employed. MW samples have increased ~ 33% of internal stresses. In contrast, CS sample has decreased ~ 28% of internal stresses (CS: 18.45 %%, MW: 27.98 %%). Therefore, this implies that part of the initial residual stresses is released after thermal cycling.

Another important result is the increase of the β-spodumene phase in both samples, CS 1200-2h and MW 1200-10, after 3600 thermal cycles. As can be observed in Table 2, the unique phase present in MW samples as-sintered, corresponds to a solid solution of β-eucryptite. However, the samples obtained by the conventional method contain a small amount of β-spodumene (0.36%). After thermal fatigue cycles, a low percentages of β-spodumene is observed in both samples (0.43% and 1.07%, conventional and microwave samples, respectively). Only the effect of stresses applied on β-eucryptite crystals due to the thermal cycling is here considered for explaining the change of β-eucryptite to β-spodumene phase, which is higher in the MW samples. Nevertheless, further work is necessary to determine if the β-spodumene phase is present at the spontaneous microcracking boundary.

3.3. Mechanical properties

Mechanical properties of CS 1200-2h and MW 1200-10 samples before and after thermal fatigue sequences are summarized in Figure 3 and Figure 4, respectively. Young's modulus (E) and hardness (H) values analyzed are averages from 250 nm to 1500 nm of depth penetration of the Berkovich tip.

Lower mechanical values obtained in CS 1200-2h as-sintered samples (68 GPa and 5.4 GPa of Young's modulus and hardness, respectively) than in the MW 1200-10 as-sintered samples (110 GPa and 7.1 GPa of Young's modulus and hardness, respectively), are due on the one hand, to the difference in density values and the other hand, the microcracks present after sintering.

After thermal fatigue cycles, hardness values of both samples decrease. In the CS 1200-2h samples, decrease is slightly until 3600 cycles (4.6 GPa), but this value is low (only 15%) in comparison with the MW 1200-10 samples (18%). The weakening effect of heat-treatment can be explained on the basis of the occurrence of new microcracks [29].

An interesting data is the different evolution of the elastic properties depending on the sintering method used to obtain the samples. Young's modulus value for CS 1200-2h samples increases with thermal cycles up to 3600 cycles (78 GPa). The lower temperature used in thermal fatigue cycles (400 ºC) may help to relieve the initial stresses, and may be the cause of the increase of the Young's modulus value in this CS samples [29].

The value of Young's modulus of MW 1200-10 samples decreases more sharply in the first 800 cycles of thermal fatigue, from 110 GPa to 92 GPa, and then the value is stable. This decrease in elastic properties is closely related to the higher percentage of

stress that has resulted in an increase of microcracks in the grains of the MW material, provoked by thermal cycling. In the MW 1200-10 samples, which have been obtained by non-conventional heating, the fatigue life behavior carried out in a conventional furnace could lead to a completely different microstructural evolution. Moreover, the higher percentage of stress has resulted in an increase of microcracks in the grains of the MW material, resulting in turn a decrease of the mechanical properties. Therefore, the final properties after thermal fatigue test for the samples obtained by conventional and non-conventional methods are different.

3.4. Dilatometric properties

The effect of internal stresses on dilatometric properties of the samples obtained by conventional and microwave, as-sintered and after thermal cycles, has been investigated. The coefficient of thermal expansion (CTE referred to 25 ºC) of conventional and microwave samples before and after thermal fatigue is presented in Figure 5. The temperature range in this measurement, -100 to 400 ºC, includes cryogenic temperatures due to the spatial applications of β-eucryptite materials such as potential substrate in space satellites' mirrors.

Some authors affirm that the CTE decreases abruptly from a small positive to a large negative value with the existence of microcracking [9,12]. According to the results of dilatometric curves that are shown in Figure 5, average CTE values in the whole range of temperatures for materials as-sintered are: $(0.1 \pm 0.8) \times 10^{-6}\ K^{-1}$ for CS and $(-1.3 \pm 0.8) \times 10^{-6}\ K^{-1}$ for MW samples. In spite of having more microcracks in as-sintered CS samples, the MW samples show more negative CTE values [13]. The presence of microcracks is not the only reason for the more negative CTE. It also depends on the sintering conditions employed. As proposed by Ramalingam et al. [2] this effect may be

attributed to stoichiometry/composition difference, variation in processing conditions (sintering/crystallization parameters) and Li-disorder process, in addition to the grain size (and thereby microcracking). Thus, the most negative CTE values for microwave sintered samples, may be due to Li positional disordering and flattening of the tetrahedral sheets in the structure via tetrahedral tilting [8].

In both cases, CS and MW samples, thermal fatigue cycling resulted in a decrease in the values of CTE to more negative values. CTE value of CS samples was initially positive, it decreased to a negative value abruptly after 3600 cycles $(-7.2 \pm 0.9) \times 10^{-6}\ K^{-1}$. The decrease is more moderate in the case of microwave-sintered samples $(-2.7 \pm 0.3) \times 10^{-6}\ K^{-1}$.

In summary, thermal fatigue cycles have caused an increase in the internal stresses of the material, leading to the breakdown of the grains in the microwave-sintered samples. The mechanical and thermal properties have decreased due to the emergence of microcracks. In the case of the samples obtained by the conventional method, thermal cycles have caused a release of internal residual stresses of the samples, resulting in a slightly improved Young's modulus value. However, the thermal properties have been highly affected adversely. The main usefulness of β-eucryptite materials is due to their high dimensional stability with temperature. In this regard, microwave sintered samples exhibit more stable thermal behavior throughout their lifetime.

This is the first time that the result of different thermal fatigue cycles on microcracking and residual stresses of samples obtained by different heating technologies is shown in the literature. Its practical consequence should be taken into account if this type of β-

eucryptite material, is to be used in the development of applications, which combine both low thermal expansion and excellent mechanical properties.

4. Conclusions

The thermal and mechanical behavior of β-eucryptite materials obtained by different sintering techniques, conventional and microwave, has been studied before and after subjecting the samples to severe thermal fatigue cycles.

Thermal fatigue cycles have resulted in an increase in the internal stresses of the microwave-sintered samples, leading to grain rupture. The mechanical properties have decreased due to the appearance of spontaneous microcracks. In the conventional samples, thermal cycles have caused a release of internal residual stresses, resulting in a slightly improved mechanical value (Young's modulus).

The appearance of microcracks in the structure of the microwave samples, and their increase in the conventional samples, has resulted in a more negative thermal expansion coefficient of both samples. However, the decrease has been more moderate in the samples sintered by microwave technology. Therefore, the microwave-sintered samples showed greater dimensional stability over time and throughout their lifetime than conventional sintering method.

Acknowledgements

A. Borrell, acknowledges the Spanish Ministry of Science and Innovation for a *Juan de*

la Cierva contract (JCI-2011-10498) and the Polytechnic University of Valencia (UPV) for financial support received under project SP20120677. The authors would like to thank the SCSIE team of the University of Valencia.

References

[1] Bruno G, Garlea VO, Muth J, Efremov AM, Watkins TR, Shyam A. Microstrain temperature evolution in b-eucryptite ceramics: Measurement and model. Acta Mater 2012;60:4982-96.

[2] Ramalingam S, Reimanis IE. Effect of Doping on the Thermal Expansion of b-Eucryptite Prepared by Sol-Gel Methods. J Am Ceram Soc 2012;95:2939-43.

[3] King DS, Fahrenholtz WG, Hilmas GE. Microstructural effects on the mechanical properties of SiC-15 vol% TiB_2 particulate-reinforced ceramic composites. J Am Ceram Soc 2013;96:577-83.

[4] Seymour KC, Kriven WM. Synthesis and thermal expansion of beta-eucryptite powders produced by the inorganic-organic steric entrapment method .J Am Ceram Soc 2014;97:3087-91.

[5] Bao Y, Yang J, Qiu Y, Song Y. Space and time effects of stress on cracking of glass. Mater Sci Eng A 2009;512:45-52.

[6] Shyam A, Muth J, Lara-Curzio E. Elastic properties of b-eucryptite in the glassy and microcracked crystalline states. Acta Mater 2012;60:5867-76.

[7] Ogiwara T, Noda Y, Shoji K, Kimura O. Low-Temperature sintering of high-strength b-eucryptite ceramics with low thermal expansion using Li_2O-GeO_2 as a sintering additive. J Am Ceram Soc 2011;94:1427-33.

[8] García-Moreno O, Fernández A, Khainakova S, Torrecillas R. Negative thermal expansion of lithium aluminosilicate ceramics at cryogenic temperatures. Scr Mater 2010;63:170-3.

[9] Moya JS, Verduch AG, Hortal M. Thermal expansion of beta-eucryptite solid solution. Trans British Ceram Soc 1974;76:177-8.

[10] García-Moreno O, Kriven WK, Moya JS Torrecilllas R. Alumina region of the litium aluminosilicate system: a new wimdow for temperature ultrastable materials design. J Am Ceram Soc 2013;96:2039-2041.

[11] Reimanis IE, Seick C, Fitzpatrick K, Fuller ER, Landin S. Spontaneous Ejecta from b-Eucryptite Composites. J Am Ceram Soc 2007:90:2497-501.

[12] Pelletant A, Reveron H, Chêvalier J, Fantozzi G, Blanchard L, Guinot F, Falzon F. Grain size dependence of pure β-eucryptite thermal expansion coefficient. Mater Lett 2012;66:68-71.

[13] Benavente R, Salvador MD, García-Moreno O, Peñaranda-Foix FL, Catalá-Civera JM, Borrell A. Microwave, Spark Plasma and Conventional Sintering to Obtain Controlled Thermal Expansion β-Eucryptite Materials. Int J Appl Ceram Technol 2015;12[S2]:E187-E193.

[14] Benavente R, Salvador MD, Peñaranda-Foix FL, García-Moreno O, Torrecillas R, Borrell A. Microwave technique: An innovated method for sintering β-eucryptite ceramic materials. Adv Sci Technol 2014;88:43-8.

[15] Benavente R, Borrell A, Salvador MD, García-Moreno O, Peñaranda-Foix FL, Catala-Civera JM. Fabrication of near-zero thermal expansion of fully dense β-eucryptite ceramics by microwave sintering. Ceram Inter 2014;40:935-41.

[16] Cheng J, Agrawal D, Zhang Y, Roy R. Microwave sintering of transparent alumina. Mater Lett 2002;56:587-92.

[17] Mizuro M, Obata S, Takayama S, Ito S, Kato N, Hiraia T, Sato M. Sintering of alumina by 2.45 GHz microwave heating. J Eur Ceram Soc 2004;24:387-91.

[18] Sandovl ML, Talou MH, Souto PM, Kiminami RH, Camerucci MA. Microwave sintering of corderite precursor green bodies prepared by starch consolidation. Ceram Inter 2011;37:1237-43.

[19] Cheng Y, Sun S, Hu H. Preparation of Al_2O_3/TiC micro-composite ceramic tool materials by microwave sintering and their microstructure and properties. Ceram Inter 2014;40:16761-6.

[20] Oghbaei M, Mirzaee O. Microwave versus conventional sintering: A review of fundamentals, advantages and applications. J Alloys Comp 2010;494:175-89.

[21] Rybakov KI, Olevsky EA, Krikun EV. Microwave sintering: Fundamentals and modeling. J Am Ceram Soc 2013;96:1003-20.

[22] Plaza-Gonzalez PJ, Canos AJ, Catala-Civera JM, Gutierrez-Cano JD. Complex impedance measurement system around 2.45 GHz in a waveguide portable system; presented at the 13th International conference on microwave and RF heating, Toulouse, September 5, pp. 290-3, 2011.

[23] Oliver WC, Pharr GM. An improved technique for determining hardness and elastic modulus using load and displacement sensing indentation experiments. J Mater Res 1992;7:1564-83.

[24] Rietveld HM. A profile refinement method for nuclear and magnetic structures. J Appl Crystal 1969;2:65-71.

[25] Rodriguez-Carvajal J. Full Prof Program. Collected Abstracts of Powder Difraction Meeting, 127-8, Tolousse, France, 1990.

[26] Cullity BD. Elements of X-Ray Diffraction. 2nd ed., Addison-Wesley, Reading, MA pp. 284-92, 1978.

[27] Stokes AR, Wilson AJC. The diffraction of X-rays by distorted crystal aggregates – I. Proc Phys Soc 1944;56:174-81.

[28] De Keijser TH, Langford JI, Mittemeijer EJ, Volgels AB. Use of the Voigt function in a single-line method for the analysis of X-ray diffraction line broadening. J Appl Crystal 1982;15:308-14.

[29] Bush EA, Hummel FA, High-Temperature Mechanical Properties of Ceramic Materials: II, Beta-Eucryptite. J Am Ceram Soc 958;41:189.

Figure captions:

Figure 1. FE-SEM images of fracture surface of samples sintered by CS 1200-2h and by MW 1200-10 with 0, 800 and 3600 thermal fatigue cycles. Microcracks are market with arrows.

Figure 2. Observed (dotted) and calculated (solid) X-ray diffraction profiles for samples sintered by CS 1200-2h and by MW 1200-10 as sintered and with 3600 thermal fatigue cycles. Tic marks below the diffractograms represent the allowed Bragg reflections of β-eucryptite (blue) and β-espodumene (red). The residuals lines are located at the bottom of the figures.

Figure 3. Young's modulus and hardness as a function of depth for the samples sintered by conventional, before and after thermal fatigue.

Figure 4. Young's modulus and hardness a function of depth for the samples sintered by microwave, before and after thermal fatigue.

Figure 5. Coefficient of thermal expansion of samples sintered by CS 1200-2h and by MW 1200-10 with 0, 800, 1800 and 3600 thermal fatigue cycles.

Table 1. Grain size of CS 1200-2h and MW 1200-10 samples before and after thermal fatigue cycles.

Thermal fatigue cycles		0	800	1800	3600
Grain size (μm)	CS 1200-2h	3.4 ± 0.9	3.5 ± 0.7	3.4 ± 0.9	3.7 ± 0.9
	MW 1200-10	2.2 ± 0.9	2.3 ± 0.7	2.3 ± 0.6	2.2 ± 0.7

Table 2. Selected data from X-ray powder diffraction studies of samples sintered by CS 1200-2h and by MW 1200-10, as-sintered and with 3600 thermal fatigue cycles.

	CS-1200-2h as-sintered		**CS-1200-2h 3600 cycles**		**MW-1200-10 as-sintered**	**MW-1200-10 3600 cycles**	
Symmetry	*Hexagonal*	*Tetragonal*	*Hexagonal*	*Tetragonal*	*Hexagonal*	*Hexagonal*	*Tetragonal*
Space group	P $6_4$22	P 4_32_12	P $6_4$22	P 4_32_12	P $6_4$22	P $6_4$22	P 4_32_12
a=b (Å)	10.5229	7.5871	10.5068	7.6036	10.5101	10.5300	7.5661
c (Å)	11.1102	7.5871	11.1586	9.1021	11.1399	11.0794	9.1132
V (Å)	1065.44	523.73	1066.80	526.23	1065.67	1063.91	521.69
$\rho_{theoretic}$ (g/cm^3)	2.3557		2.3527		2.3552	2.3591	
R_{Bragg}	4.8	43.8	12.3	44.9	5.6	7.8	37.3
R_p; R_{wp}	11.7; 12.9		6.9; 9.0		14.0; 14.4	6.0; 8.4	
χ^2	6.5		7.5		5.5	5.5	
wt. %	99.64	0.36	99.57	0.43	100	98.93	1.07
Strain (%%)	25.34		18.45		21.54	27.98	

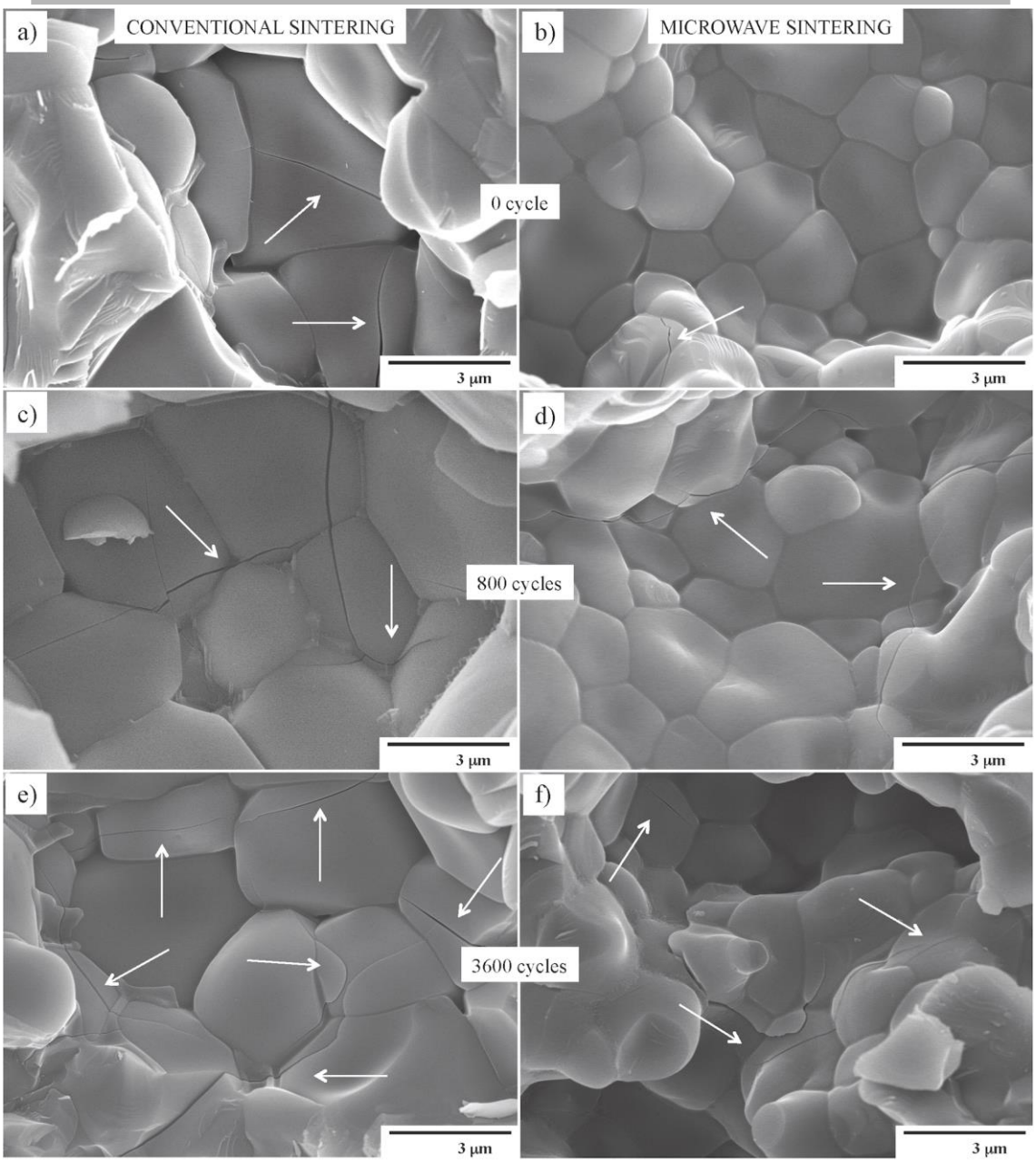

fig 1

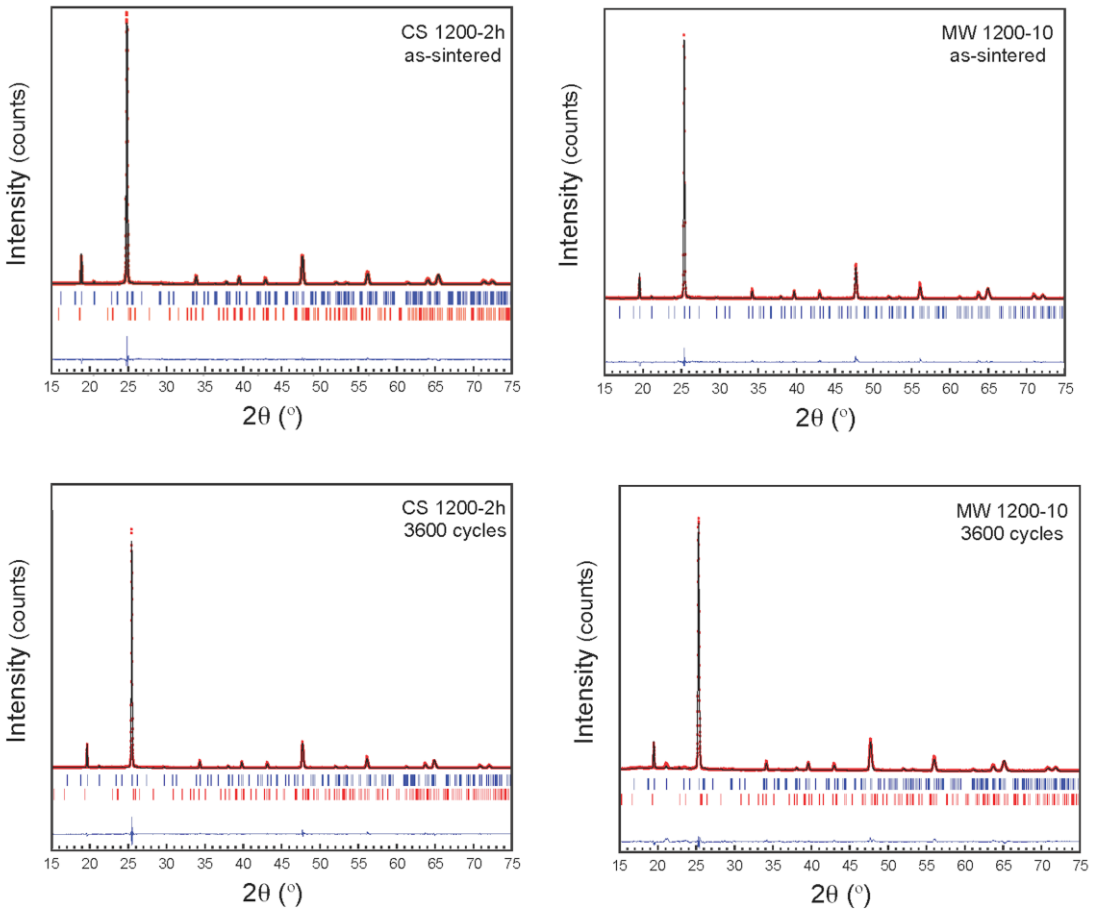

fig 2

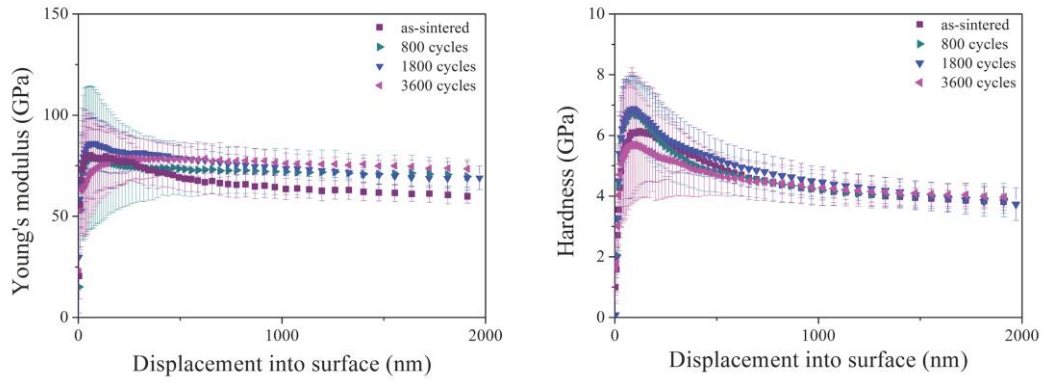

fig 3

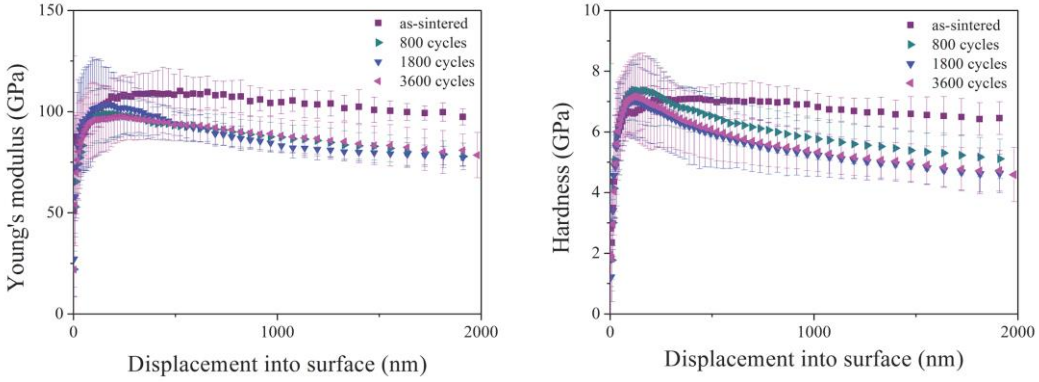
Young's modulus (GPa)
Displacement into surface (nm)
Hardness (GPa)
Displacement into surface (nm)
as-sintered
800 cycles
1800 cycles
3600 cycles

fig 4

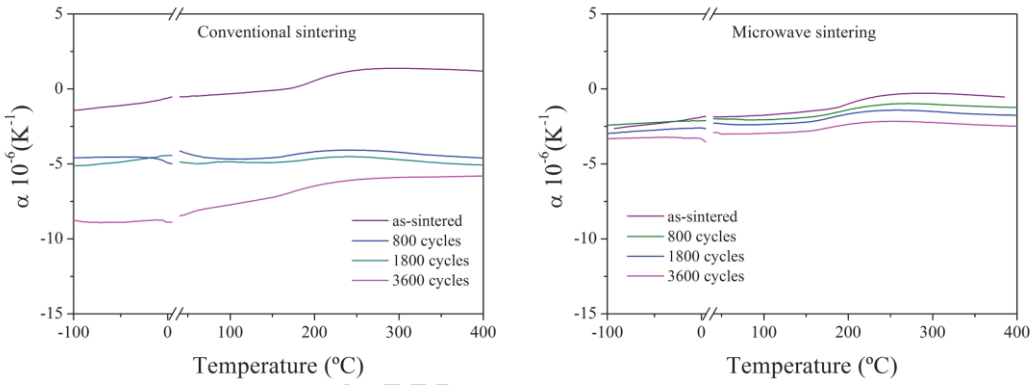
Conventional sintering
Microwave sintering
α 10^-6 (K^-1)
Temperature (ºC)
as-sintered
800 cycles
1800 cycles
3600 cycles

fig 5